Proceedings of ECOS 2021 - The 34th International Conference on
Efficiency, **C**ost, **O**ptimization, **S**imulation and **E**nvironmental Impact of Energy Systems
June 27-July 2, 2021, Taormina, Italy

Exploring the Tradeoff between Installed Capacity and Unserved Energy in Rural Electrification

Alejandro Soto[a], Sergio Balderrama[b], Evelyn Cardozo[c], Fernandez Miguel[d], Zambrana Jaime[e] and Sylvain Qouilin[f]

[a] Universidad Mayor de San Simon, Cochabamba, Bolivia, 201508362@est.umss.edu
[b] University of Liege, Liege, Belgium, slbalderrama@doct.uliege.be
[c] Universidad Mayor de San Simon, Cochabamba, Bolivia, evelyncardozo.r@fcyt.umss.edu.bo
[d] ENERGETICA, Cochabamba, Bolivia, miguel@energetica.org.bo
[e] Universidad Mayor de San Simon, Cochabamba, Bolivia, jaimezambranavargas@gmail.com
[f] University of Liege, Liege, Belgium, squoilin@ulg.ac.be

Abstract:
With the current goal of reaching a 100% electrification rate of the world population, the importance of PV/battery or solar home systems (SHS) grows as the one of the most viable solution for the most remote and scattered communities. Their modularity and capacity to harvest local resources is particularly relevant for that purpose. The stochasticity of solar energy and of the demand can however lead to energy shortages in the most critical periods of the day, while an over-sized system represents an important increase in the levelized cost of energy (LCOE). To capture these dynamics and the trade-off between installed capacity and lost load probability (LLP), 16 different demand scenarios are modeled and analyzed. An optimal size for SHS is determined using a linear programming model with different levels of LLP in each scenario. The Demand time series are constructed using a stochastic demand generator that simulates the behavior of each appliance on a household. The information to create the base-case scenario was obtained with field surveys of a rural community in Cochabamba, Bolivia (Raqaypampa). Each scenario has different combinations of appliances, including the intensive use of radio to comply with guidelines of remote education (due to the COVID-19 crisis). The result shows that there is a high reduction of the LCOE in the lower range of LLP. This reduction reaches a breaking point where a higher LLP does not represent a significant further reduction of the LCOE. An empirical mathematical formulation is proposed to calculate this inflection point and a Pareto front plotted to assess the tradeoff between quality of service and LCOE.

Keywords:
Energy integration, Energy planning, Renewable Energy, Rural electrification, Solar Home System

1. Introduction

The world faces crucial challenges in terms of the increasing energy requirement [1], this will contribute to a greater emission of greenhouse gases [2]. The decarbonization of energy production is one of the great challenges of the century [3]. All societies are going through a drastic change regarding energy sources [4]. The energy needs of humans have a notable influence on social development [5, 6] and the provided energy quality. This has major consequences in rural areas of developing countries [7]. The use of Solar Home Systems (SHS) and an improvement in service, may imply a significance reduction in fuel costs [8], these savings that would allow the development of small and medium-sized production units, increasing production rates and diversifying them [9]. One of the problems due to COVID-19 has been the implementation of distance education [10]. This would imply an increase in demand. The present work develops the implications that distance education may have on unsupplied energy.
Rural electrification is essential for socio-economic development in emerging countries [11]. Although energy is used for different basic purposes, it is not enough to improve the rural economy and make profound social change. Isolated micro grids offer a higher level of access to energy; however, in remote populated rural areas, this solution could be a costly investment [7]. On the other hand, SHS may be a feasible solution to achieve 100% rural electrification in Bolivia [12]. The problem resides in many techno economic factors [13] associated with consumption limitations to cover basic needs and future scaling with increasing demand [7]. This growth is associated with the adoption of new household appliances due to the increase in the economy and the number of Productive Units [14] (PU). The Productive Energy Use (PUE) is one of the main reasons for the change in energy sources [15]. The present work presents an alternative method to achieve the optimal sizing for the specific case of SHS, in contrast to the already existing method applied to MicroGrids [16].

It is important to take into account the potential impacts of the SHS limitations may have in different household activities [17] and therefore in universal access to energy [18]. This paper exposes the relationship of the

Levelized Cost of Energy (LCOE) and the Net Present Cost (NPC) as a function of the of Loss of Load Probability (LLP) in different scenarios that contemplate the specific presence of electronic devices for common and PUE. Through optimization, it will allow to analyze the trade-off between the energy unsupplied and the LCOE, allowing to evaluate the impact that this could have in the life of inhabitants of households.

2. Methods

From a sequential point of view, for the analysis of the influence of the unsupplied energy in relation to the activities of each household, it is necessary to collect sufficient input data that allow assessment closer to reality for the specific case of a remote population. With all time series obtained, it is pertinent to optimize the SHS that will allow to be no notable influence on the LCOE and the NPC without compromising the energy unsupplied (breaking point), this iteratively can take a few seconds or several days depending on the steps to use for this method. In this context, the estimation of the breaking point takes up simpler alternatives that allow the modular segregated analysis of appliances, and, therefore, of the activities associated with each household.

The RAMP tool used to obtain the random and unpredictable time series of demand contemplates a single level associated with the type of appliance of a specific type of user [19]. These users can be classified depending on energy needs, based on socio-economic indicators. For the analysis of the techno-economic indicators of the SHS, the use of a technique based on machine learning has been foreseen [20]. For its optimization under certain boundary conditions, the variability of the LCOE and the NPC is identified as a function of the probability that the system cannot supply a fraction of the demand. Likewise, characteristics of the functional relationship (breaking point) are identified using the Maximum Distances Method (MDM) [21], which allow resizing to specific conditions for analysis of the limit influence of the energy not supplied on the activities of each household.

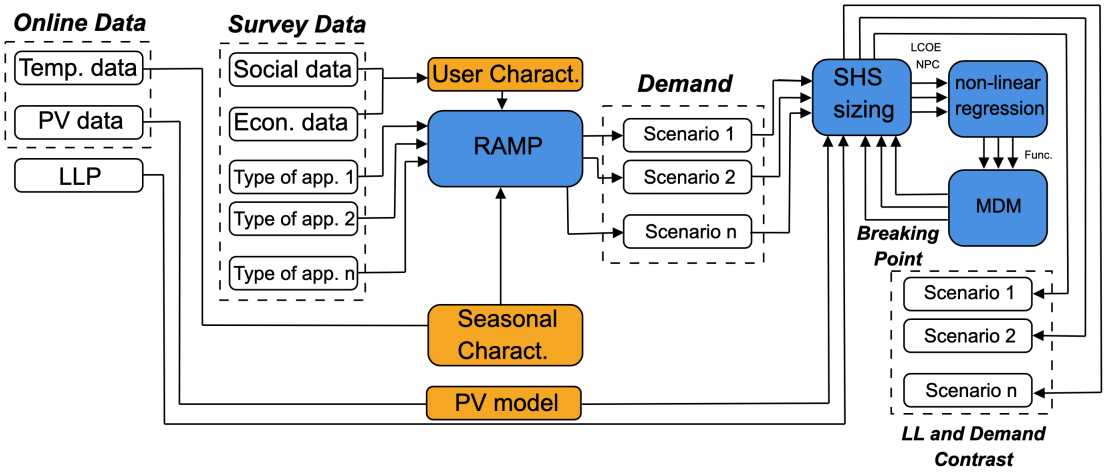

Figure 1: Flow Information Diagram.

2.1. RAMP for estimating Demand.

The estimation of the demand per household and per appliance was carried out using a bottom-up stochastic model. For this, it is chosen to classify the users, likewise this model requires information on the characteristics of the electrical appliances (approximate nominal power). This information is based on probabilities of use in certain time intervals, limit and representative values of use, as well as frequency of use (for household appliances for occasional use). The data collected allows the generation of time series per minute, the randomization is independent in each layer. RAMP allows the individual evaluation of each appliance (even those of occasional use) and user in an amount of days defined.

The characterization of the types of user is dependent on the type of analysis of interest, in this case the type of electrical appliance, the economic activity and the monetary income per household are the most relevant aspects. The daily load curve [22] (occasional and typical), are proposed based on estimates within the context of the case study. Although the number of users whose energy consumption is similar to a productive unit in defined periods of the year is scarce, the number of users is not a layer to take into account in the stochastic model for estimating average demand in the SHS. The representativeness of the demand curves throughout the year should consider the appropriate treatment on the individual daily estimates. Likewise, the use of

optional stochastic models of the equipment with variable power (refrigerator and freezer) has been taken into consideration. The nominal load of this type of equipment is determined by the temperature at a certain time.

2.2. Hourly PV energy generation estimates

The estimation of the photovoltaic energy available in the geographic location of analysis requires time series data of the total radiation; incident per surface (I_t^{glo}) and the temperature of the photovoltaic cell (T_t^{PV}). The phenomenon of diffusion, refraction and typical reflection of electromagnetic waves applied to solar radiation on the ground is defined by the Equation 1. The ground is essentially a surface with inclination β, where I_t and I_g is the horizontally incidence radiation on a surface and reflected radiation respectively and ρ is the diffuse refractance of the environment.

$$I_g = I \cdot \rho \cdot \frac{1 - cos\beta}{2} \tag{1}$$

With the ambient temperature (T_t^{amb}) at defined time interval t at a set nominal cell temperature ($NOCT$) it is possible to calculate the outlet temperature of the photovoltaic cell (T^{PV}). The Equation 2 defines the relationship of the parameters to be used.

$$T_t^{PV} = T_t^{amb} + \frac{NOCT - 20}{800} \cdot I_t^{glo} \tag{2}$$

One of the greatest difficulties is the accessibility to empirical data on ambient temperature and surface irradiation in remote areas. Due to this, it is available to use approximate data from a web platform “renewables.ninja”. This platform has a MERRA-2 database to generate time series of temperature and irradiation at any latitude and altitude in the world. The time series obtained have the time step of one hour, allowing the user to define the inclination angles [23, 24]. Once the synthetic time series is obtained, the cell output data is calculated. The calculated time series allow the resolution of a five parameter model (Equation 3) for estimate the effective irradiance (I_{eff}) incident on a surface applied to a circuit [25, 26].

$$I_{eff} = I_b \cdot R_{beam} \cdot K_{\tau\alpha} + I_d \cdot K_{\tau\alpha,d} \cdot \frac{1 + \cos(\beta)}{2} + \rho_g \cdot I \cdot K_{\tau\alpha,g} \cdot \frac{1 - \cos\beta}{2} \tag{3}$$

Where K_i are the incidence angle modifiers for direct undispersed radiation b in determined value of relation between the radiation of the beam on the inclined surface and that of a horizontal surface (R_{beam}) at any angle ($i = \tau\alpha$), and at 58^o ($\tau\alpha, d$ and $\tau\alpha, g$) for diffuse and ground reflected radiation.
The generalization [27] of photovoltaic cells with equivalent circuits (De Soto Single Diode Model, Equation 4) allows the estimation of the photovoltaic energy available for various commercial modules in any location [26, 28].

$$I = I_L - I_o \left(e^{\frac{V+IR}{a}} - 1 \right) - \frac{V + IR_s}{R_{sh}} \tag{4}$$

The five parameters are the ideality factor (a), light current (*lightcurrent*), diode reverse saturation current (I_o), series resistance (R_s) and shunt resistance (R_{sh}).

2.3. Sizing tool

The tool used uses two linear optimization steps for isolated hybrid Microgrids. Although this tool can enter data from different energy sources, the first optimization step of the SHS would only focus on the flow of solar energy in different scenarios (s). The next optimization step is based on the energy flow through the system components in a defined time interval (t). That fraction of the energy supplied (E^{re}) by the source that cannot be supplied to the system ($E^{re,u}$), depends on intrinsic aspects of the unit, such as efficiency (η^{re}) and the yield (N^{re}).

The optimization relies on the modeling of input ($E^{bat,ch}$) and output ($E^{bat,dis}$) flow energy from the battery bank. This is based on technical characteristics of this SHS component such as the efficiencies of charge (η^{ch}) and discharge (η^{dis}), in addition to the nominal capacity (C^{bat}). The optimization considers limit values of the state of charge ($P^{bat,ch}$ y $P^{bat,dis}$), which allow the optimization to carry out energy dispatch, with a charge balance.

The boundary conditions for the SHS are given by an energy balance (5) that considers that portion of the energy that cannot be supplied (LL, E^{LL}) by the system with respect to a demand (D). And that energy that cannot be consumed or stored ($E^{Curtailment}$).

$$D_{s,t} = E_{s,t}^{re} - E_{s,t}^{bat,ch} - E_{s,t}^{bat,dis} + E_{s,t}^{LL} + E_{s,t}^{Curtailment} \tag{5}$$

Therefore, the first boundary condition is probabilistically related to the loss of load (Lost Load Probability, LLP). The probability of occurrence of this event in this case depends on each scenario, in this study it was

based on the determination of the variability of the result of the objective function as a function (Equation 6) of the variation of this probability. The restriction imposed for the minimum portion of energy from non-deliverable energy sources, and a minimum of energy in the battery bank in case of a blackout, considering the independence of the battery with respect to the SHS (N^{bat}) and the minimum percentage of renewable energy (I^{re}). Likewise, the minimum flow of energy for the battery is established in order to reduce the cost that this implies, the sizing tool is capable of generating the time series associated with the assigned cost. The objective function of optimization consists of minimizing the total investment cost for the project (NPC), which is the addition of the project investment (*Inv*) and the costs of supplying the annual demand (*YC*), in conjunction with the discounts (e) in the year (y).

$$Inv + \sum_{s=1}^{S} \left(\sum_{y=1}^{Y} \frac{YC_s}{(1+e)^y} \cdot I_s^{occurrence} \right) \tag{6}$$

It is logical to expect that the *Inv* of the SHS will depend on the technical characteristics of the components of the units. For a more detailed understanding of the optimization model, it is recommended to refer to [29] and observe in detail based on the description made which are the terms to simplify.

2.4. Non-linear regression

The nonlinear regression process was carried out by means of an optimization using the Levenberg-Marquardt (LM) method, essentially [30], this is preloaded in the scipy.optimize library. This algorithm is a modification of the Gauss-Newton method (Equation 7) that is based on the linearization of the residuals. The iteration will be much faster if it has points close to minimizing the sum of the least squares that will allow the problem to converge [31].

$$\delta\mu = -(J^T J)^{-1} \nabla C = -(J^T J)^{-1} J^T r \tag{7}$$

Where μ is the set of parameters, J is the Jacobian matrix that depends on the number (m and set of parameters is defined as $J_{m,\mu} = \partial r_m / \partial \mu_i$, where r are the residuals. C is the sum of frames to minimize in all parameters in the i iterations.

The SciPy library is an open source library that together with the sublibery allows the optimization of the least squares of fit of a given data series. In this case, the variability of the output techno-economic indicators of MicroGrids.py, the LCOE and NPC as a function of the LLP was analyzed (Equation 8 y 9). The variation of the indicators of interest was evidenced by iterative resizing using the optimization tool described in 2.3.. The increments used were 0.5% to 10% and 10% to 100% LLP. The functional relationship between the variables of interest corresponds to an algebraic series analogous to the simple Michaelis Menten [32] equation or Hinshelwood-Lindemann kinetic model.

$$LCOE = \frac{C_1 \, (LLP)^{C_2} + C_3}{C_4 + \sum_{i=5}^{n} C_i \, (LLP)^{C_{i+1}}} \tag{8}$$

$$NPC = \frac{A_1 \, (LLP)^{A_2} + A_3}{A_4 + \sum_{i=5}^{n} A_i \, (LLP)^{A_{i+1}}} \tag{9}$$

Where C_i and A_i are constants of the fit model for the functional relationship of the LCOE and the NPC, respectively. Note that the terms of the algebraic series can be neglected depending on the scenario to be treated. To verify the fit of the functional relationship, only the coefficient of determination (R^2) was taken as a reference of a conclusive statistical parameter, functional relationships with up to 12 statistical coefficients or parameters were used for this purpose.

This technique is based on the use of Parameter objects as variables. This method allows to improve the uncertainty after the first regression with the approximate values, the library has several models adaptable to different types of curves. The first regression is based on the Bayesian method (Equation 10) of data whose characteristics that allow the handling of any distribution of modeling uncertainty. This first regression allows the generation of the Markov and Monte Carlo chain (MCMC) and nested sampling [33].

$$p(\mu|D) \, \alpha \, p(D|\mu) \cdot p(u) \tag{10}$$

Simple Bayesian theory states that there is a direct relationship between the probability of agreement between the set of parameters with respect to the input data ($p(\mu|D)$) and the probability of likelihood between the input data and the estimates ($p(D|\mu)$) and the anticipated probability of the parameters ($p(\mu)$). The MCMC algorithm is based on the generation of a chain from a continuous random variable whose probability density

is proportional to the function to be adjusted. The chain of points generated is analyzed integrally on the random variable, taking this as a reference of the expected value or the estimated variance. The Monte Carlo method allows these variables to be correlated, making it necessary to calculate the errors of the mean values. Throughout the relationship of the chain, the condition of proportionality is maintained with the given function [34].

2.5. Maximum Distance Method (MDM)

Obtaining the point of maximum curvature represents the change in trend of the analysis parameters with respect to LL, this through the method proposed in [21]. The geometry of the estimated function found is used to obtain the point of maximum curvature that represents the change in trend of the analysis parameters with respect to LL Figure 3). Where a secant line is drawn with the extreme values of LLP (0% and 100%), the function that describes the secant line is illustrated in Equation 11.

$$y_s = a_o + a_1 x_s \tag{11}$$

It is expected that the functional relationships are at a greater distance with respect to this line drawn. For this purpose, is drawn a perpendicular line to a y_s (Equation 12). With the established perpendicularity condition, the relationship between the slopes of the lines can be found (Equation 13).

$$y_d = b_o + b_1 x_s \tag{12}$$

$$b_1 = \frac{-1}{a_1} \tag{13}$$

If several lines are drawn perpendicular to y_s, the slopes (b_i) of the lines drawn would be constant. This condition allows an iterative process to be carried out where the variations would be referred to the parameter b_o of the line.

The line y_d intercepts with the function (LCOE and NPC) and with y_s, the result obtained is two points that allow finding a distance with the general equation of distances in a plane, with the Cartesian information of the points obtained (14).

$$d_j = \sqrt{\left(y_{j,d} - y_{s,d}\right)^2 + \left(x_{j,d} - x_{s,d}\right)^2} \tag{14}$$

Where j are the two study indicators (LCOE and NPC). The iterative process would consist of two systems of equations to find the points of intersection. The nonlinear system will be solved by Python's symbolic numeric solver [35].

3. Case of Study

The selected case study is a SHS from the "indigenous rural native autonomous territory of Raqaypampa", in the department of Cochabamba located in the Plurinational State of Bolivia. The information related to the inputs of the demand estimation model was obtained based on surveys of a sample of fifty people, the surveys were carried out in the period from 10/03/2019 to 10/10/2019) [36].

3.1. Meteorological data and demand data

For the case study, demand curves and meteorological data are not available. For this reason, the open-source RAMP tool was used to estimate the demand information to size and optimize the SHS. Regarding meteorological information (photovoltaic energy in the area and temperature), the online platform renewables.ninja (https://www.renewables.ninja/) has been used. The input data for the platform were latitude (-18.1891201) and longitude (-65.3847939) in the local time from 01/01/2018 00:00:00 to 12/31/2018 23:00:00.

3.2. User characterization

To establish the base and scenarios with productive activities. These types of scenarios contemplate the use of high consumption appliances associated with the generation of seasonal or regular income. It is common to observe this type of behavior in rural areas in the absence of legally constituted businesses, those activities must necessarily provide a service to more than a household [37]. Families have been characterized based on socioeconomic factors,identified in the surveys performed. A simple conditional criterion and estimates [38,39] of net income per household was proposed. The factors analyzed were the type of economic activity per person in the household, net income, rate of electricity consumption, total number of people in the household, number of people who generate income, existence of high-consumption appliances, number of rooms per household, building materials.

Based on these data, the 50 families surveyed could be characterized into two big groups ($A = 44$ and $B = 6$). From now on, each household will be called "user". These groups have as their main indicator the type of economic activity that the entire household. The power data for each appliance was based on characteristics described in the surveys and making assumptions based on the *DaftLogic* database [40].

3.3. Demand scenarios

The devices of low power and daily use are proposed as a starting point to establish the scenarios. The rest of the scenarios are proposed (Sn, n = 1, 2, . . . , 16) in a modular way with each one of the appliances of occasional and atypical use (Tables 1 and 2).

Table 1: Definition of the modular scenarios from base scenario proposed for user A. (*) Variable power and cycle of use; (**) Atypical Use; (***) Seasonally variable power [36]. The Baseline Scenario for user A considers: 3 Indoor Bulbs, 1 Outdoor Bulb, 1 Radio, 1 TV, 2 Phone Charger, 1 Water heater, 1 Mixer*.

Appl.	S1	S2	S3	S4	S5	S6	S7	S8	S9
Freezer	1*			1	1*				1*
Fridge	1	1	1*						1*
Welder						1***			1***
Grinder							1***		1***
Industrial Dryer								1	1

Table 2: Definition of the modular scenarios proposed for user B. (*) Variable power and cycle of use; (**) Atypical Use; (***) Seasonally variable power [36]. The Baseline Scenario for user B considers: 3 Indoor Bulbs, 1 Outdoor Bulb, 1 Radio, 1 TV, 2 Phone Charger.

Appl.	S10	S11	S12	S13	S14	S15	S16
Water pump		1					1
Blender				1			1
Iron**					1		1
Washing machine**	1						1
Mill**						1	1
DVD			1				1

To propose the scenarios that consider mixed distance education (through community radios) according to the guidelines established by local authorities. [41, 42]. A continuous educational radio program by levels has been assumed over a period of 30 minutes [43], based on earlier protocols in the region (Peru). The temporal gradients were added to the base scenario based on the number of students according to the surveys, with a maximum of 3 and 5 people for the type of users A and B respectively, thus proposing 8 scenarios (CSn, n = 1, 2, 3. . . , 8).

4. Results and Discussion

4.1. Estimated annual demand

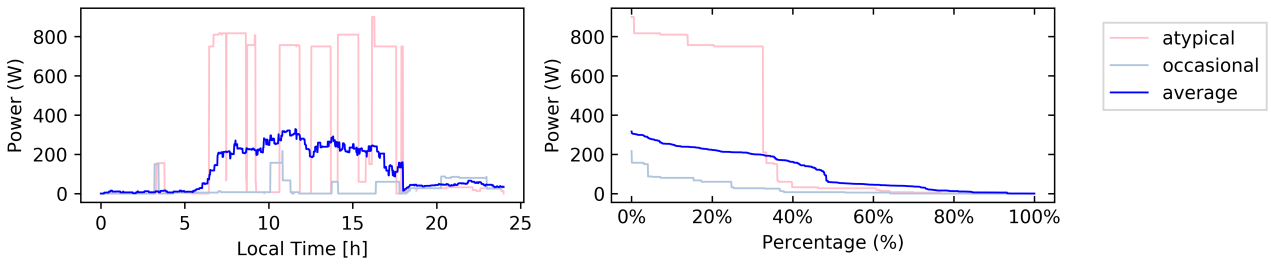

Figure 2: Left;Average demand per day for March, comparison between the average per time change and the typical and occasional demand curves for the S7 scenario. Right; Normalized curves of average, typical and occasional demand during March for the S7 scenario.

With all the input data of the RAMP tool defined, the average monthly demand for one year was estimated for the proposed scenarios. Although, the robustness of the model is not altered by the individual estimation of users or appliances. The presentation of the average demands (per minute) is not representative. The scenario S7 (Figure 2) is taken as a reference because its characteristics allow to visualize an extreme case of underestimation.

4.2. Generalization based on nonlinear regression

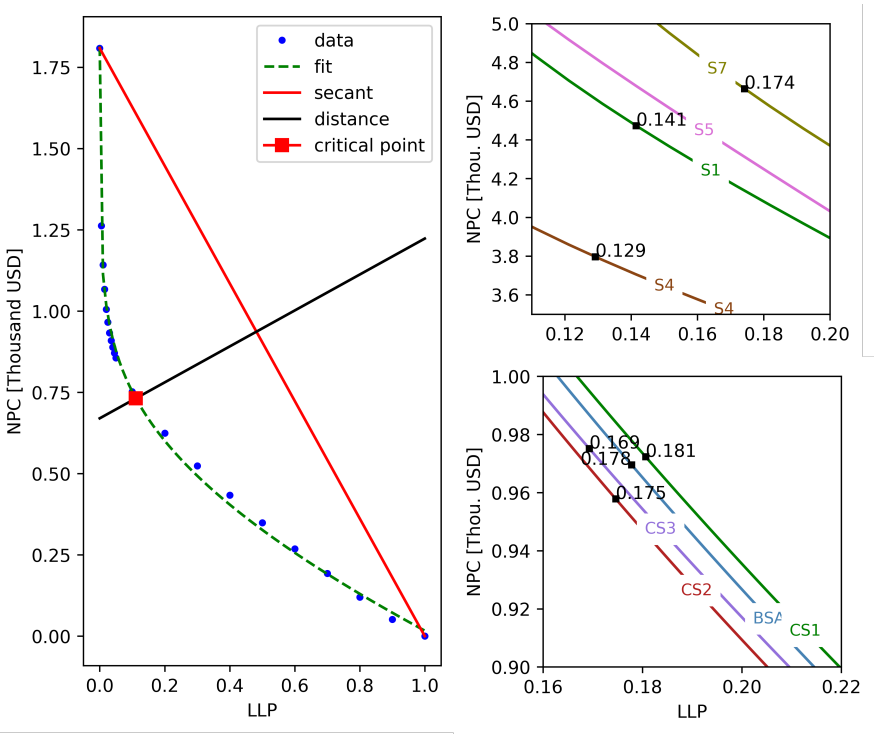

Figure 3: Left; Nonlinear adjustment of the variation of NPC as a function of LLP, graphical representation of MDM for S14. Right; Break point for the adjusted curves of NPC as a function of LLP for the some scenarios with productive activities and distance education proposed.

It has been possible to generalize the functional relationship between LCOE and NPC, and the probability of the system of not being able to supply a fraction of the required energy (LLP). The functional relationships were drawn through exploratory iterations, and the Equations 8 and 9 establishes the generalization of this exploration. In all cases, a determination coefficient greater than 0.99 was obtained. Something to take into consideration is that those scenarios with only productive activities (Tables 1 and 2), the cost of energy and the total investment cost is higher (Figure 3). The generalization extends to the proposed distance education scenarios for both indicators with respect to the indirect relationship with the number of students and the increase in the LCOE and NPC. In scenarios where demand increases, the cost of energy supply decreases, at the expense of increasing the risk of blackouts, due to the decrease in the nominal capacity of the battery bank (BNC) and NPC.

4.3. Finding the Breaking Point

Figure 3 (right) shows the critical points of some of the proposed scenarios, obtained with the MDM. Something remarkable is that the behavior not correlated with the demand of the limit values in the functions (obtained in 4.2.) extends to the breaking points.

The initial points of the iteration were given by the intersection of the secant with the functional relationship found. Note that each of the scenarios will have two critical points (optimal LCOE and NPC). The meaning of this point is the change in strategy from shaving the peak to reducing demand in other places. This lead to stop reducing the investment in technology and start reducing the operation cost (Table 3). It is important to highlight the comparative importance of the scenarios without restrictions of economic activities and most frequently the scenarios with distance education (1 student per household) for the two types of users.

4.4. LL contrast based on modular demand

With the critical point obtained in the previous section, the SHS has been resized at the point where the amount of energy supplied does not significantly affect the total investment cost of the system and the unit cost of en-

Table 3: Summary of optimization results at critical points of LCOE and NPC. CP = critical point AVG = average, SD = standard deviation, MAX = maximum, MIN = minimum, S9 = user A without restrictions, S16 = user B without restrictions.

		CP LCOE			CP NPC		
		BNC Wh	NPC K USD	LCOE USD/KWh	BNC Wh	NPC K USD	LCOE USD/KWh
USER A	AVG	1.56	3.603	0.671	1.60	3.671	0.68
	MAX	5.69	8.750	1.768	5.75	8.827	1.78
	MIN	0.47	1.017	0.384	0.45	0.982	0.38
S9		3.05	10.081	0.560	2.46	8.473	0.47
CS1		3.05	10.081	0.560	2.46	8.473	0.47
USER B	AVG	0.44	0.880	0.720	0.39	0.787	0.65
	MAX	0.85	1.648	1.120	0.54	1.112	0.76
	MIN	0.33	0.665	0.622	0.31	0.645	0.60
S16		0.70	1.397	0.727	0.67	1.362	0.71
CS4		3.05	10.081	0.560	2.46	8.473	0.47

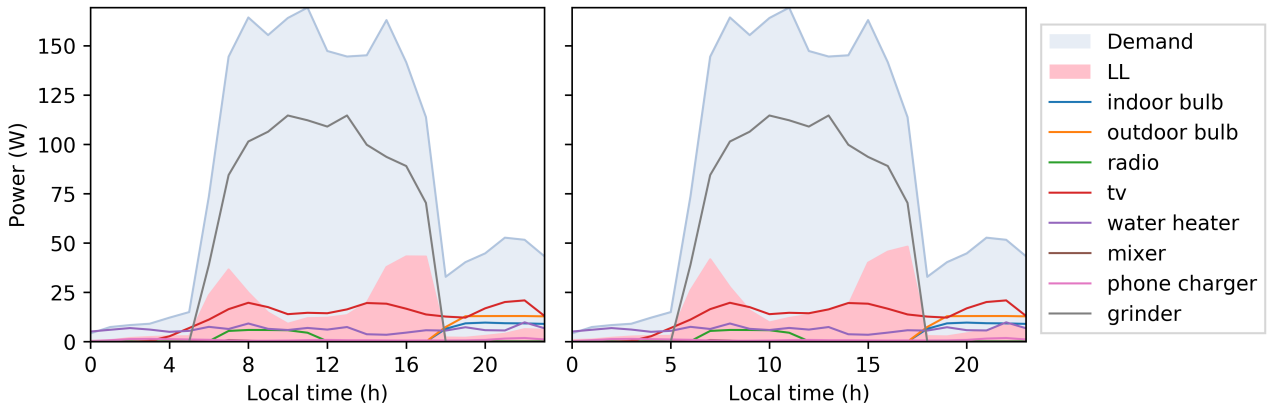

Figure 4: Average total annual demand contrasted with the modular demand of each appliance and the LL, obtained with an LLP at an optimal LCOE (left) and NPC (right) for the S7.

ergy. It is very important to analyze which equipment will be affected by the inability of the SHS to supply the total of the required demand. This incidence will allow us to observe the possible effect on productive activities (Tables 1 and 2). Likewise, in the scenarios with distance education, it allows to visualize those appliances that could be compromised.

The influence of the loss load on frequently used appliances with high energy consumption is remarkable, likewise this is explained by the behavior of the total demand of the proposed scenario, this behavior is extensible to other scenarios with activities productive with high consumption appliances such as the scenario illustrated in Figure 4, this contrast is less marked in an average representative curve. This could be explained by the greater incidence of the other more frequently used appliances on the total demand, however, during the short period of use, the system would have a drastic momentary inability to supply power to the system. Peak demand hours coincide with the operating hours of appliances involved in high-consumption productive activities around 12:00 noon. These differences are less appreciable in the scenarios with education due to the closeness in characteristics (in terms of demand) with the base scenarios. Likewise, these implications on the modular demand curves are not easily appreciable and interpretable in the unrestricted scenarios.

5. Conclusion

In this work, a sequence of steps is exposed to be able to evaluate the energy supply capacity of an SHS in a remote population of a developing country. For this purpose, each electrical appliance available in the homes and their characteristic productive use was considered. 26 scenarios were proposed, considering productive activities and distance education. The SHS were dimensioned based on the estimated demands for one year and the meteorological data obtained and calculated from the case study. Through non-linear regression based on two mathematical methods, the relationship between the techno-economic indicators of the SHS and the probability that the system was not able to supply a fraction of total demand was found. Using geometric and numerical techniques, the limit that the system will not be able to supply a certain portion of the demand without compromising the investment in the SHS and the unit price of the energy supplied was determined. At this boundary, the demand per appliance was contrasted to analyze the SHS service with respect to the energy not supplied and the individual activities of each type of household.

For the analysis case study, it was found that the relationship between the total investment cost of the SHS and the unit price of energy service has a general form, regardless of the proposed scenario. This is verifiable by a coefficient of determination greater than 0.99 in each scenario. The analysis showed that at the breaking point it would lead to stop reducing investment in technology and begin to reduce the cost of operation. Another finding is that it is necessary to schedule the demand before sizing this type of systems.

Finally, in order to ensure a good transparency, reproducibility and re-usability of this work, all the datasets, scripts and models are released under an open license and are available in the following repository: [44].

6. Acknowledgments

The authors wish to acknowledge the “Academie de recherche et d’enseignement superieur” (Belgium) and SDSN Bolivia for the financial support.

References

[1] P. A. Owusu and S. Asumadu-Sarkodie, “A review of renewable energy sources, sustainability issues and climate change mitigation,” *Cogent Engineering*, vol. 3, no. 1, p. 1167990, 2016.

[2] R. Schaeffer, A. S. Szklo, A. F. P. de Lucena, B. S. M. C. Borba, L. P. P. Nogueira, F. P. Fleming, A. Troccoli, M. Harrison, and M. S. Boulahya, “Energy sector vulnerability to climate change: a review,” *Energy*, vol. 38, no. 1, pp. 1–12, 2012.

[3] S. Pfenninger, A. Hawkes, and J. Keirstead, “Energy systems modeling for twenty-first century energy challenges,” *Renewable and Sustainable Energy Reviews*, vol. 33, pp. 74–86, 2014.

[4] E. E. S. Michaelides, *Alternative energy sources*. Springer Science & Business Media, 2012.

[5] Y. S. K. S. S. K. T. Z. P. E. G. H. S. S. C. v. S. P. M. Ottmar Edenhofer Ramón Pichs-Madruga, *Renewable Energy Sources and Climate Change Mitigation: Special Report of the Intergovernmental Panel on Climate Change*. Cambridge University Press, 2011.

[6] P. Iemsomboon, N. Tangtham, S. Kanjanasuntorn, and S. Bualert, “Modeling community quality of life indicators for developing solar home system in remote areas,” *Energy Procedia*, vol. 9, pp. 44–55, 2011.

[7] C. T. Shaw, “Assessing Feasibility of Fostering Productive Energy Use of Swarm Electrified Microgrids in Rural Communities in Developing Countries,” Master’s thesis, Universitat Politècnica de Catalunya, 2017.

[8] A. Shahsavari and M. Akbari, “Potential of solar energy in developing countries for reducing energy-related emissions,” *Renewable and Sustainable Energy Reviews*, vol. 90, pp. 275–291, 2018.

[9] L. X. Zhang, B. Song, and B. Chen, “Emergy-based analysis of four farming systems: insight into agricultural diversification in rural China,” *Journal of Cleaner Production*, vol. 28, pp. 33–44, 2012.

[10] N. Lustig, G. Neidhöfer, M. Tommasi, *et al.*, “Short and long-run distributional impacts of covid-19 in latin america,” tech. rep., Tulane University, Department of Economics, 2020.

[11] D. Lecoque and M. Wiemann, “The productive use of renewable energy in Africa,” *European Union Energy Initiative Partnership Dialogue Facility: Eschborn, Germany*, pp. 1–9, 2015.

[12] J. G. P. Balderrama, S. B. Subieta, F. Lombardi, N. Stevanato, A. Sahlberg, M. Howells, E. Colombo, and S. Quoilin, “Incorporating high-resolution demand and techno-economic optimization to evaluate microgrids into the Open Source Spatial Electrification Tool (OnSSET),” *Energy for Sustainable Development*, vol. 56, pp. 98–118, 2020.

[13] A. A. Eras-Almeida, M. Fernández, J. Eisman, J. G. Mart\'\in, E. Caamaño, and M. A. Egido-Aguilera, "Lessons learned from rural electrification experiences with third generation solar home systems in Latin America: Case studies in Peru, Mexico, and Bolivia," *Sustainability*, vol. 11, no. 24, p. 7139, 2019.

[14] R. D'Arlon, "Hybrid mini-grids for rural electrification: Lessons learned," 2014.

[15] R. A. Cabraal, D. F. Barnes, and S. G. Agarwal, "Productive uses of energy for rural development," *Annu. Rev. Environ. Resour.*, vol. 30, pp. 117–144, 2005.

[16] C. Hanley, M. Ross, R. Foster, L. Estrada, G. Cisneros, C. Rovero, L. Ojinaga, and A. Verani, "Using renewable energy for rural connectivity and distance education in latin america," in *Conference Record of the Twenty-Ninth IEEE Photovoltaic Specialists Conference, 2002.*, pp. 1481–1484, IEEE, 2002.

[17] B. Van Campen, D. Guidi, and G. Best, "Solar photovoltaics for sustainable agriculture and rural development," in *Rural Development", Fao Publication*, Citeseer, 2000.

[18] R. Ebenhoch, D. Matha, S. Marathe, P. Cortes Muñoz, and C. i Borrell, "Comparative levelized cost of energy analysis," *Energy Procedia*, vol. 80, pp. 108–122, 2015.

[19] F. Lombardi, S. Balderrama, S. Quoilin, and E. Colombo, "Generating high-resolution multi-energy load profiles for remote areas with an open-source stochastic model," *Energy*, vol. 177, pp. 433–444, 2019.

[20] S. Balderrama, W. Canedo, M. Fernandez, V. Lemort, and S. Quoilin, "Techno-economic optimization of isolate micro-grids including PV and Li-Ion Batteries in the Bolivian context," *Proceedings of ECOS*, 2016.

[21] L. H. Lorentz, R. Erichsen, and A. D. Lúcio, "Proposta de método para estimação de tamanho de parcela para culturas agr{\'\i}colas," *Revista Ceres*, vol. 59, no. 6, pp. 772–780, 2012.

[22] F. Lombardi, F. Riva, M. Sacchi, and E. Colombo, "Enabling combined access to electricity and clean cooking with pv-microgrids: new evidences from a high-resolution model of cooking loads," *Energy for Sustainable Development*, vol. 49, pp. 78–88, 2019.

[23] S. Pfenninger and I. Staffell, "Long-term patterns of european pv output using 30 years of validated hourly reanalysis and satellite data," *Energy*, vol. 114, pp. 1251–1265, 2016.

[24] I. Staffell and S. Pfenninger, "Using bias-corrected reanalysis to simulate current and future wind power output," *Energy*, vol. 114, pp. 1224–1239, 2016.

[25] W. F. Holmgren, C. W. Hansen, and M. A. Mikofski, "pvlib python: a python package for modeling solar energy systems," *The Journal of Open Source Software*, vol. 3, p. 884, 2018.

[26] W. De Soto, S. A. Klein, and W. A. Beckman, "Improvement and validation of a model for photovoltaic array performance," *Solar energy*, vol. 80, no. 1, pp. 78–88, 2006.

[27] J. A. Duffie and W. A. Beckman, *Solar engineering of thermal processes*. John Wiley & Sons, 2013.

[28] "California energy commission pv library." `https://www.gosolarcalifornia.ca.gov/equipment/pv_modules.php`. Accessed: 2019-02-28.

[29] S. Balderrama, F. Lombardi, F. Riva, W. Canedo, E. Colombo, and S. Quoilin, "A two-stage linear programming optimization framework for isolated hybrid microgrids in a rural context: The case study of the "el espino" community," *Energy*, vol. 188, p. 116073, 2019.

[30] M. Newville, T. Stensitzki, D. B. Allen, M. Rawlik, A. Ingargiola, and A. Nelson, "Lmfit: Non-linear least-square minimization and curve-fitting for python," *Astrophysics Source Code Library*, pp. ascl–1606, 2016.

[31] M. K. Transtrum and J. P. Sethna, "Improvements to the levenberg-marquardt algorithm for nonlinear least-squares minimization," *arXiv preprint arXiv:1201.5885*, 2012.

[32] M. Sakoda and K. Hiromi, "Determination of the best-fit values of kinetic parameters of the michaelis-menten equation by the method of least squares with the taylor expansion," *The Journal of Biochemistry*, vol. 80, no. 3, pp. 547–555, 1976.

[33] A. Rokem, "A short course about fitting models with thescipy. optimizemodule," *Journal of Open Source Education*, vol. 2, no. 16, p. 16, 2018.

[34] C. Geyer, "Introduction to markov chain monte carlo," *Handbook of markov chain monte carlo*, vol. 20116022, p. 45, 2011.

[35] A. Meurer, C. P. Smith, M. Paprocki, O. Čertík, S. B. Kirpichev, M. Rocklin, A. Kumar, S. Ivanov, J. K. Moore, S. Singh, *et al.*, "Sympy: symbolic computing in python," *PeerJ Computer Science*, vol. 3, p. e103, 2017.

[36] M. Fernández F, E. Cardozo R, J. Zambrana V, G. Peña, S. Balderrama, C. Sánchez, A. Soto, and S. Quoilin, "PROPUESTAS ACCIONABLES," *Atlas Municipal de los Objetivos de Desarrollo Sosotenible en Bolivia 2020*, 2020.

[37] T. Muñoz Máximo, I. Ocampo Fletes, and F. Parra Inzunza, "Socioeconomic characterization of the family production unit and the importance of the cultivation of chia (Salvia hispanica L.) in the municipalities of Atzitzihuacán and Tochimilco, Puebla, Mexico," *Acta universitaria*, vol. 29, 2019.

[38] E. Bernal, B. Muriel, and G. Olivarez, "Pobreza, ingresos laborales y trabajo en Bolivia," tech. rep., Development Research Working Paper Series, 2015.

[39] G. Mena and W. Jiménez, "Trazando l{\'\i}neas: estimación de la canasta básica de alimentos y l{\'\i}neas de pobreza en Bolivia para el periodo 1999-2012," *Revista Latinoamericana de Desarrollo Económico*, no. 20, pp. 111–148, 2013.

[40] Daft Logic, "Information appliance power consumption," 2019.

[41] Ministerio de Educación, "Resolución Viceministerial No. 125-2020," 2020.

[42] Ministerio de Educación-Estado Plurinacional de Bolivia, "RESOLUCIÓN MINISTERIAL N° 001/2021. SUBSISTEMA DE EDUCACIÓN ALTERNATIVA Y ESPECIAL," 2021.

[43] UNICOM – MINEDU, "MINISTERIO DE EDUCACIÓN: CLASES EN LAS CIUDADES CAPITALES SE INICIARÁN BAJO LA MODALIDAD A DISTANCIA," 2021.

[44] "Permanent repository for the scripts and data sets for the paper: Exploring the tradeoff between installed capacity and unserved energy in rural electrification." `https://github.com/CIE-UMSS/Tradeoff-between-Installed-Capacity-and-Unserved-Energy`. Accessed: 2021-03-02.